Improved Truss Model for Design of Welded Steel Moment-Resisting Frame Connections

Jaswant N. Arlekar[1] and C. V. R. Murty[2]

Abstract: This paper presents results of finite element analysis of 18 strong-axis steel welded beam–column subassemblages with connection reinforcement. For the type of connection configuration considered, Federal Emergency Management Agency (FEMA) recommends that the connection forces be obtained by locating the plastic hinge at one-third depth of beam away from the end of connection reinforcement region. Also a recent study pointed the location of plastic hinge to be at a distance of depth of beam from the column face. However, the present study shows that the plastic hinge is located at one-half depth of beam away from the end of connection reinforcement region. It is observed that the connection design forces obtained from the present study are higher as compared to those obtained using the FEMA recommendations. The paper also presents a noniterative procedure for the design of beam-to-column connections using a truss for obtaining connection forces, which uses this location of the plastic hinge.

DOI: 10.1061/(ASCE)0733-9445(2004)130:3(498)

CE Database subject headings: Steel; Connections, welded; Seismic design; Finite element method; Beam columns.

Introduction

The design of connections for steel beam-to-column joints is based on capacity design concept, wherein connections are designed for forces corresponding to beam overstrength capacity. Also, the conventional procedure for design of connection elements at the beam-to-column moment–shear connections is based on simplified beam-bending theory, wherein it is assumed that the beam-end moment is transferred to the column through beam flanges alone and the beam-end shear through beam web. However, recent studies (Lee et al. 1998, 2000) have shown that the above design assumptions are not realistic. The actual stress field near the beam-to-column joint region is not properly reflected in the above-simplified approach for the design of connections elements. It was shown that the truss analogy model (Goel et al. 1996) can be used to represent the flow of forces near the connection region.

This paper presents the results of nonlinear finite element analyses of strong-axis exterior steel beam-to-column subassemblages with connection reinforcement; the connection reinforcement consists of beam–flange cover plates and vertical rib plates. Based on the principal stress fields in beam-to-column subassemblages, the truss analogy model is improved. Also, based on the capacity design concept a noniterative procedure is outlined for the design of connection elements. The proposed procedure is itself used in the design of the connection elements for the beam-to-column subassemblages studied.

[1]PhD, 5706 Trailview Ct. A11, Frederick, MD 21703.

[2]Professor, Dept. of Civil Engineering, Indian Institute of Technology Kanpur, Kanpur, India 208016. E-mail: cvrm@iitk.ac.in

Note. Associate Editor: Takeru Igusa. Discussion open until August 1, 2004. Separate discussions must be submitted for individual papers. To extend the closing date by one month, a written request must be filed with the ASCE Managing Editor. The manuscript for this paper was submitted for review and possible publication on March 30, 2000; approved on March 19, 2003. This paper is part of the ***Journal of Structural Engineering***, Vol. 130, No. 3, March 1, 2004. ©ASCE, ISSN 0733-9445/2004/3-498–510/$18.00.

Moment Transfer Joints

For steel moment-resisting frames, the seismic design philosophy recommends the use of strong-column weak-beam concept in which the frame members are proportioned such that the plastic hinges occur in the beams rather than the columns. This requirement imposes severe strength and deformation demands on the beam-to-column connections. The performance of steel moment-resisting frame (MRF) buildings during the 1994 Northridge earthquake has emphasized the vulnerability of moment-resisting connections during strong earthquake shaking. Although there was no loss of life during the Northridge earthquake due to collapse of steel MRF buildings (EQE 1994), the performance of steel MRF buildings was not satisfactory. Many low- and medium-rise steel moment-frame buildings sustained structural damage at the beam-to-column joints. These buildings were designed and detailed according to the then existing building code requirements, which were intended to ensure ductile performance of the buildings during major earthquakes (Krawinkler and Popov 1982). Damage to moment frames included brittle failures of beams flange weld connections, and fracture of column flanges including portions of column web, particularly near the beam bottom flange. Some bolts of shear tabs were also damaged along with the tearing of shear tab and the fillet weld from the column face (Miller 1998). Failures of welded connections have been reported in buildings located as far as 30 km from the epicenter [National Institute of Standards and Technology (NIST) 1994]. This is an issue of concern as the Northridge earthquake was just a moderate size earthquake (magnitude 6.8 on Richter scale).

Prescriptive Moment Connection

The connection scheme used most in steel MRFs from mid 1960s to 1994 is known as the prescriptive moment connection (Fig. 1). This connection scheme was adopted by the 1988 Uniform Building Code (UBC) based on limited tests conducted to qualify the connections (Saunders 1998). It was assumed that total plastic moment (M_p) is transferred through the full-penetration welds at

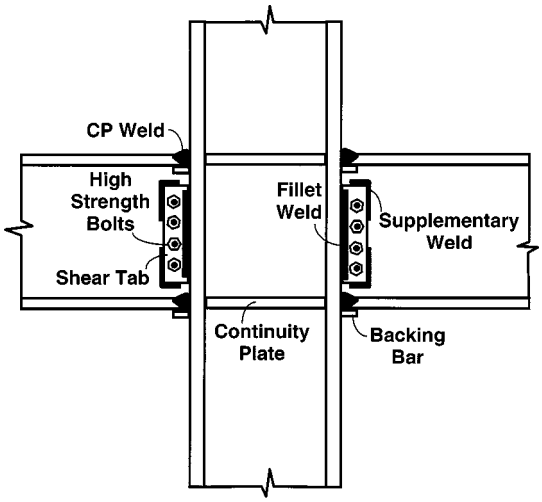

Fig. 1. Prescriptive moment connection specified between beam and column in steel moment-resisting frame buildings

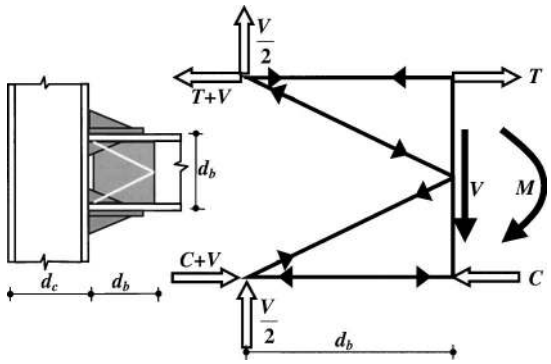

Fig. 2. Beam–column subassemblage showing location of truss analogy model and connection elements and geometry and force of truss analogy model for flow of forces near connection reinforcement region (Lee et al. 2000)

the end of the beam flanges, and the corresponding shear force (V) through the shear tabs and high strength bolts at the end of the beam web.

The prescriptive moment connections were deemed as sufficiently ductile to develop full plastic moment capacity in the beam and thereby to perform very well during strong ground shaking. These connections were economical, and therefore widely used in steel MRF buildings in high seismic zones. However, during the Northridge earthquake, the prescriptive moment connection performed poorly and was immediately withdrawn by UBC. Many such connections sustained extensive damage, particularly in the complete penetration weld region even before any inelasticity was developed (Roeder 1998; Saunders 1998).

The experimental investigations after the Northridge earthquake showed that the prescriptive moment connections were indeed inadequate to sustain the deformation demands during strong earthquake shaking (Sabol et al. 1996; Englehardt and Sabol 1998; Malley 1998). Further, it was also observed that connection failures during the Northridge earthquake were not just due to poor quality of welding, but also due to three-dimensional restraint in the connection region, which do not allow the expected ductile yielding of the beam flanges (Miller 1998). It was understood that it is not possible to form energy dissipating plastic hinges at the column face, as the restraints in this region do not allow ductile yielding of the beam. The restraint provided by the column flange makes the beam-end connection vulnerable to brittle fracture (Miller 1998). Thus, the current design philosophy of steel beam-to-column connections requires that during strong seismic shaking (1) the connections remain elastic and (2) the energy dissipating plastic hinges be formed away from the column face [Engelhardt and Sabol 1998; Federal Emergency Management Association (FEMA) 2000]. The inelasticity is concentrated at a predetermined location in the beam, away from the column face.

According to von Mises criterion, both normal stress (σ_{xx}) and shear stress (τ_{xz}) participate in yielding the section. σ_{xx} is more effective in yielding the portions away from the neutral axis, and τ_{xz} in yielding the portions near the neutral axis. A plastic hinge is formed in the beam when inelasticity spreads by flexural yielding of flanges and shear yielding of web. Therefore, the plastic hinge is not a single point in the beam, but is spread along a small length of the beam span and across the full depth of the beam cross section. It is known that welds are vulnerable to brittle fracture when subjected to large deformations; this is counterproductive to good inelastic behavior. Steel, on the other hand, is a ductile material, and it also strain hardens giving additional strength even after yielding. Further, the formation of plastic hinge results in large deformation in the hinge portion. Therefore, the design strategy is to push the potential plastic hinge away from the connections (welds, cover plates, and rib plates), into the span of the beam. This is achieved by reinforcing the connection region. However, it is important to recognize the following conflicting demands:

1. The plastic hinge region should be sufficiently away from the restraint at the column face to allow for the plastification in the beam; and
2. The design moment for the connection is amplified with increase in the distance of plastic hinge from the face of the column.

Under the large lateral loading on the frame, the joint panel zone (JPZ) in the column section is subjected to very high shear stresses. Inelastic yielding of JPZ is expected to dissipate the input seismic energy in the frames with prescriptive moment connections. However, excessive yielding of the JPZs caused kinking in the columns and imposes severe deformation demands on the beam-to-column connections (Schneider and Amidi 1998). This was identified as one of the main reasons for the fracture of the complete penetration welds in the prescriptive moment connections during the 1994 Northridge earthquake. Further, excessive distortions of the JPZs due to yielding may result in undesirable storey drifts, and thereby adversely affect the behavior of connections near the joint (Krawinkler and Popov 1982).

Truss Analogy Model

Experimental and analytical studies (e.g., Goel et al. 1996; Lee et al. 1998) have shown that the beam stress field postulated by classical Bernoulli hypothesis is not valid for regions near the joint. A truss analogy model was used to represent the flow of forces in this region (Fig. 2) (Goel et al. 1997; Lee et al. 2000).

In the truss analogy model, a K-truss is used to represent the flow of forces, which starts at the face of the column. Based on these forces, a connection design scheme was proposed consisting of cover plates and vertical rib plates (Goel et al. 1996) (Fig. 2). However, in this method, the design forces for the individual connection reinforcement elements, namely, the beam-flange

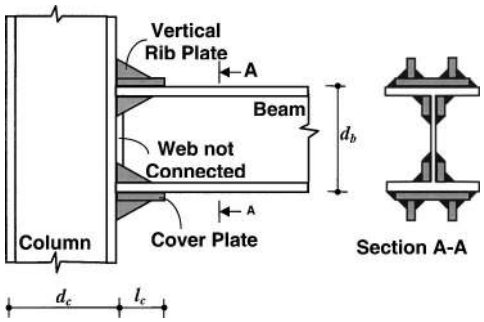

Fig. 3. Beam–column subassemblage configuration showing location of connection elements and relative position of beam and column used in this study

cover plates and vertical rib plates, are arbitrarily assigned. Further, the presence of connection reinforcement is not reflected in the location of the K-truss; the K-truss starts at the column face (Fig. 2). However, the strength of the beam near the column face is increased by the presence of the connection reinforcement elements. During strong seismic shaking, the bending moment is largest in the beam near the column face. But, because the beam strength is increased near the column face by the presence of connection reinforcement, yielding will not be initiated there. Instead, yielding will start immediately adjacent to the beam reinforcement region, where the section has lesser strength. Thus, it is only appropriate to start the K-truss at the end of the connection reinforcement region rather than at the face of the column. Provisions of FEMA 267 for buildings with low gravity loads also suggest that the truss may be assumed to span over a distance of $d_b/3$ from the edge of the connection reinforcement region (FEMA 1995). Further, the truss analogy model states that the length of the truss is equal to the depth (d_b) of the beam (Lee et al. 2000), which is inconsistent with the observations of the present study.

Present Study

In the present study, welded steel beam-to-column connections are studied through a typical exterior beam-to-column subassemblage made of AISC *W* sections and conforming to the strong-column weak-beam design philosophy. The sudden change in geometry at the column face and the consequent stress concentration there is avoided by reinforcing the joint region with cover plates and vertical rib plates. In the connection considered: (1) the beam flanges are butt welded to the column flange; (2) the cover plates are fillet welded to the beam flange and butt welded to the column; and (3) the vertical rib plates are fillet welded to the cover plates and butt welded to the column (Fig. 3). This connection scheme is similar to that proposed in the literature (Goel et al. 1996) (Fig. 2). A possible sequence of fabrication for this connection scheme, using down-hand and vertical welds, is

1. Shop weld the bottom outer rib plates to the bottom cover plate with fillet welds.
2. Shop weld the bracket developed in step (1), to the column with CJP welds.
3. Position the beam on this bracket prepared in step (2), and field weld the beam flange to the cover plate with down-hand fillet welds.
4. Field weld both the beam flanges to the column flange with down-hand complete joint penetration (CJP) welds.
5. Field weld the top cover plate to the beam flange with down-hand fillet welds, and then to the column flange with down-hand CJP weld.
6. Field weld the top outer rib plates to the top cover plate column with vertical fillet welds, and then to the column flange with vertical CJP welds.
7. Field weld the bottom inner rib plates to the column flange with vertical CJP welds, and to the beam flange and web with down-hand fillet welds.
8. Field weld the top inner rib plates to the column with vertical/overhead CJP welds, and to the beam flange and web with vertical fillet welds.

Nonlinear finite element analyses are performed for 18 beam-to-column subassemblages using the finite element analysis software *ABAQUS* [Hibbitt, Karlsson & Sorensen Inc. (HKS) 1996]. The geometry and support conditions of these subassemblages studied are shown in Fig. 4(a). The properties of the *W* sections used in the beam-to-column subassemblages are listed in Table 1. The subassemblages are discretized using eight-noded solid elements, with three translational degrees of freedom per node; a finer mesh is used to model the connection region. The finite element model of a typical beam-to-column subassemblage (beam $W21\times142$, column $W24\times160$) is shown in Fig. 4(b), along with details of the mesh near the top rib plate [Fig. 4(c)]. The beam web is not connected to the column flange.

In all 18 subassemblages, the connections are designed for the strut and tie forces obtained by assuming that the connection truss: (1) begins at the end of the connection reinforcement region, (2) has a K-type configuration, and (3) has dimension of $d_b/2$ along the beam span. The detailed procedure employed for the design of the connection elements is enumerated later in this paper. Since both the beam-to-column subassemblage and the loading are symmetric about the vertical plane (say $y=0$ plane) passing through the center of the beam web and column web, only one-half of the subassemblage is modeled with *y* symmetric constraints applied to all nodes on the $y=0$ plane. The top and bottom ends of the column stub are fixed. Monotonically increasing displacement is applied to the tip of the beam.

Improved Truss Model

Under vertical downward displacement of the beam tip, the region above the neutral axis is subjected to tensile normal stresses (σ_{xx}) and shear stress (τ_{xz}) as shown in Fig. 5; a tie can be used to represent the resultant of these two. Similarly, the region below the neutral axis is under the action of compressive normal stresses (σ_{xx}) and shear stress (τ_{xz}); a strut can be used to represent the resultant of these two. Stress contours in the joint region for 0.33, 1.00, and 4% drift of the subassemblage with $W21\times142$ beam and $W24\times160$ column are shown in Fig. 6.

The reinforcing effect of cover plates and the vertical rib plates near the column face pushes the critical section for yielding into the span of the beam. Fig. 7 shows the variation of normal stress (σ_{xx}) in the flange of beam along the length of the beam for 0.33, 1.00, and 4.00% drift; σ_{xx} is maximum at the end of the connection reinforcement region. The distribution of shear stress (τ_{xz}) near the end of the reinforced region is reversed (Fig. 5) with τ_{xz} being a minimum at the neutral axis, as observed in the previous study (Lee et al. 1998). At the end of the connection reinforcement region, both σ_{xx} and τ_{xz} are maximum near the beam flanges (Figs. 5 and 6). The principal stress is inclined at an angle less than 45° to the horizontal; this inclination depends on the intensity of normal stresses. The high normal and shear stresses at

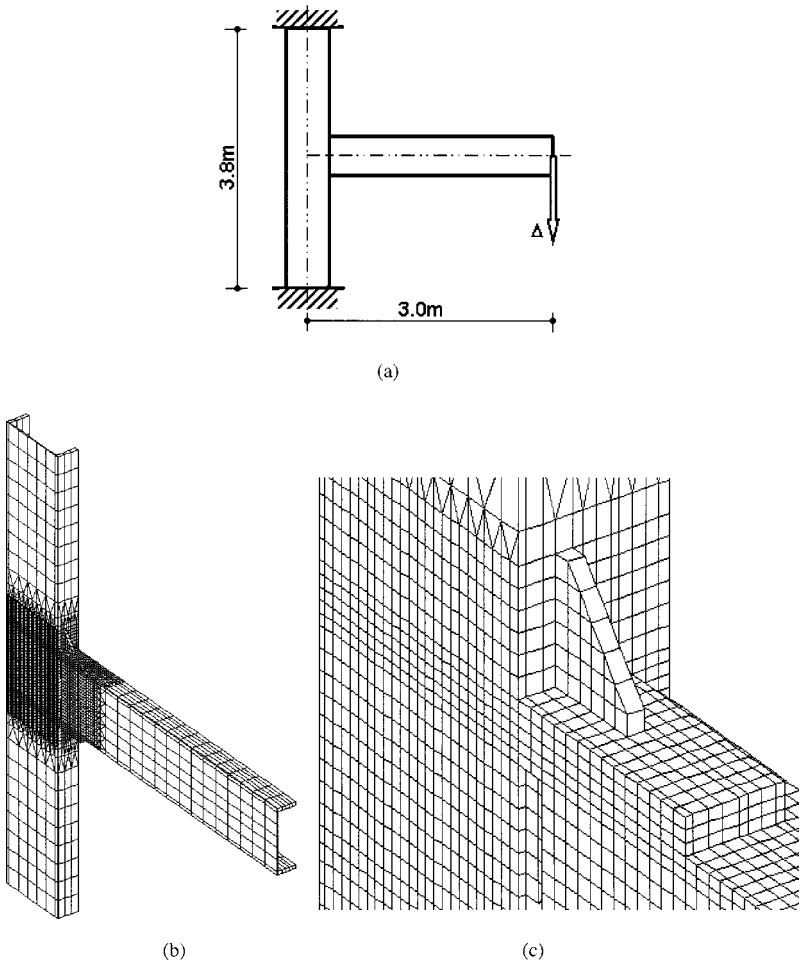

Fig. 4. (a) Beam–column subassemblage considered in this study, (b) finite element model of symmetric half of beam–column subassemblage (beam $W21\times142$, column $W24\times160$), and (c) details of finite element model showing discretization of connection reinforcement region

this section result in the highest von Mises stress in the beam flange. This suggests that during strong shaking, yielding will initiate in the beam flange at the end of the connection reinforcement region and, under increased deformation, the inelasticity will spread outwards along the beam flange and towards the neutral axis in the web.

The shear stress distribution at a section away from the end of the connection reinforcement region confirms the validity of the postulated classical Bernoulli theory, with maximum stress at the neutral axis. Further, the shear stress contours for the beam-to-column subassemblages considered in this study agree with those observed in the previous study (Lee et al. 1998); maximum shear stress occurs at the beam neutral axis for sections away from the connection reinforcement region, and near the beam flange for sections near the connection reinforcement region. The beam section at neutral axis is under the state of pure shear and the principal stress is inclined at 45° to the horizontal. Thus, in the beam portion adjoining the connection reinforcement region, the inclination of principal stresses is oriented at an angle less than 45° near the beam flanges, and approaches 45° towards the neutral axis by the end of the K-truss; the principal stress trajectory in the K-truss region is therefore not a straight line (Fig. 5). However, for the purpose of estimating the connection design forces, it is assumed that a linear truss is formed beyond the end of connection reinforcement region.

The first point along the centerline of the beam beyond the connection reinforcement region, at which the shear stress is maximum, is the point where the shear yielding will initiate. This point is called the truss point. Fig. 8 shows the distribution of shear stress (τ_{xz}) along the neutral axis of the beam for the example subassemblage (beam $W21\times142$ and column $W24\times160$). The distance of the truss point from the end of connection reinforcement region is called the length (l_t) of the truss. The intensity of shear stresses in the column panel zone, connection reinforcement region, and the beam region are for 0.33, 1.00, and 4.00% drift levels, and are listed in Tables 2, 3, and 4, respectively. Fig. 9 shows the results for the variation of l_t with beam depth (d_b) for 0.33, 1, and 4% drifts of the 18 subassemblages studied. The best linear fits of this data are

$$\frac{l_t}{d_b}=\begin{cases}0.57 & \text{for } 0.33\% \text{ drift}\\ 0.36 & \text{for } 1.00\% \text{ drift}\\ 0.35 & \text{for } 4.00\% \text{ drift}\end{cases} \tag{1}$$

With increase in drift, i.e., increased inelastic deformation, the truss point moves towards the column. Fig. 9 also shows the curve corresponding to $l_t/d_b=0.5d_b$. Clearly, assuming the truss point to be located at $0.5d_b$ from the end of the connection reinforcement region gives an upper bound. In the 18 subassemblages studied, the above observation is consistent with the original as-

Table 1. Properties of *W* Sections Used in Beam-to-Column Subassemblages

Sr. No.	Column	Beam	d_b	b_{bf}	t_{bf}	t_{bw}	Z_b in.^{4}	M_{pb}/M_{pc}	Cover plate			Rib plate		
									L	B	T	L	H	T
1	$W36\times300$	$W33\times240$	851	406	36	21	918.2	0.732	425	260	65	235	300	30
2	$d_c=932$	$W27\times177$	694	358	30	18	556.9	0.444	345	235	55	135	170	30
3		$W21\times142$	545	334	28	17	357.0	0.284	270	220	45	130	155	20
4		$W16\times96$	415	294	22	14	186.0	0.148	200	200	40	45	80	16
5		$W12\times58$	310	254	16	9	86.5	0.069	150	190	30	25	40	16
6	$W33\times240$	$W27\times177$	694	358	30	18	556.9	0.607	345	235	50	155	180	30
7	$d_c=851$	$W18\times114$	469	301	25	15	247.9	0.270	230	200	40	110	130	16
8		$W12\times58$	310	254	16	9	86.5	0.094	155	190	30	25	40	16
9	$W27\times144$	$W24\times160$	628	358	29	17	463.7	0.833	310	240	50	115	150	25
10	$d_c=694$	$W21\times142$	545	334	28	17	357.0	0.641	270	220	45	125	150	20
11		$W16\times96$	415	294	22	14	186.0	0.334	200	200	40	40	75	16
12	$W24\times160$	$W21\times142$	545	334	28	17	357.0	0.770	270	220	45	120	145	20
13	$d_c=628$	$W18\times114$	469	301	25	15	247.9	0.535	230	200	40	110	125	16
14		$W12\times58$	310	254	16	9	86.5	0.187	155	190	30	25	40	16
15	$W21\times142$	$W21\times142$	545	334	28	17	357.0	1.000	270	220	45	120	145	20
16	$d_c=545$	$W16\times96$	415	294	22	14	186.0	0.521	200	200	40	40	75	16
17	$W18\times114$ $d_c=469$	$W12\times58$	310	254	16	9	86.5	0.349	155	190	30	25	40	16
18	$W16\times96$ $d_c=415$	$W16\times96$	415	294	22	14	186.0	1.000	200	200	40	40	70	16

sumption made in the design of connection elements that the truss point is at $0.5d_b$ from the connection reinforcement region. This assumption is also consistent with the stress flow as shown in Fig. 5.

Transverse beam load versus drift curves for the 18 subassemblages studied are shown in Fig. 10. The transverse beam load is normalized with P_{pb}, the load corresponding to the beam plastic capacity (M_{pb}), given by

$$P_{pb}=\frac{M_{pb}}{L-\left(\frac{d_c}{2}+l_c\right)} \tag{2}$$

where L=distance between the column centerline and beam tip; d_c=column depth; and l_c=length of the connection reinforcement region along the beam from the column face. Drift of the subassemblage is defined as

$$\%\ \text{drift}=\frac{\Delta}{L}\times100\% \tag{3}$$

where Δ=beam tip displacement. From Fig. 10, beam moments corresponding to 0.33% drift are substantially small; P/P_{pb} ratios are less than 0.6, and the response of the subassemblage is elastic. For 1% drift, the beam plastic moment is mobilized; P/P_{pb} ratios are close to 1.0. For 4% drift, the P/P_{pb} ratios are as high as 1.2, and the beam is in the strain-hardening range.

Based on the above observations, an improved truss model is proposed. This model overcomes the shortcomings of the truss location and length in the earlier truss analogy model (Lee et al. 2000). The salient features of the improved truss model are (Fig. 11):

1. *Configuration*: a K-truss adequately represents the transfer of beam shear from the web to the connection elements;
2. *Location*: the K-truss starts at the end of connection reinforcement region and spans into the beam; and
3. *Geometry*: the length l_t of the K-truss is $d_b/2$.

In the proposed model, the moment amplification due to the formation of plastic hinge away from the face of the column is more accurately considered. Further, because the beam web does not transfer shear to the face of the column, it is not essential to connect the beam web and the column flange for transfer of design shear. However, the beam web may be connected through

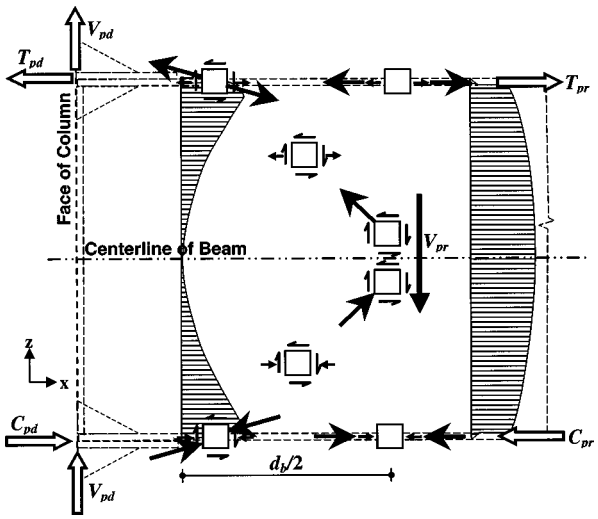

Fig. 5. Maximum principal stress directions in connection reinforcement region based on observed shear stress distribution for beam-to-column connection configuration studied

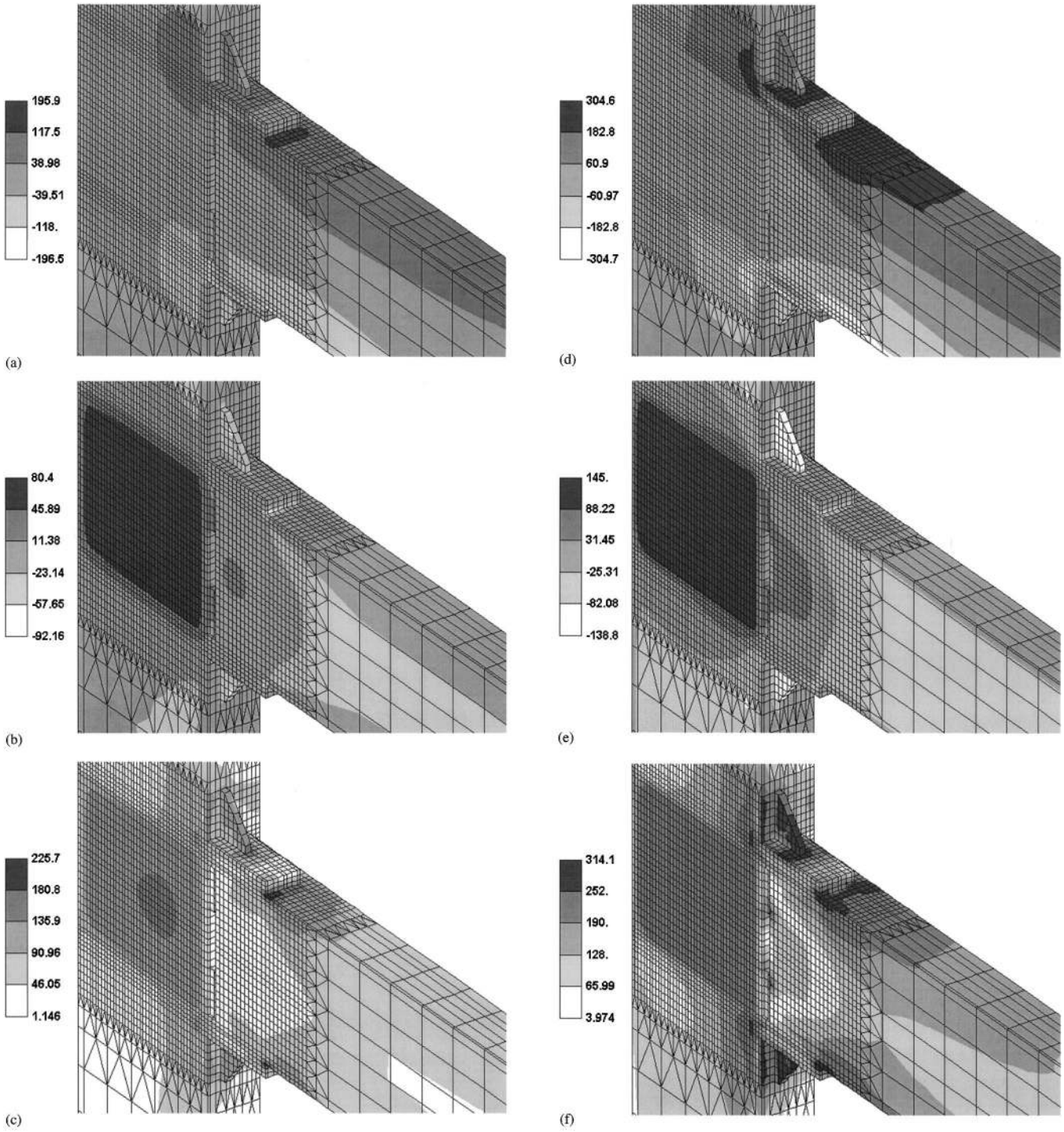

Fig. 6. (a) Normal stress contours (MPa); (b) shear stress contours (MPa); and (c) von Mises stress contours (MPa) in connection region for 0.33% drift of beam–column subassemblage studied (beam $W21\times142$ and column $W24\times160$). (d) Normal stress contours (MPa); (e) shear stress contours (MPa); and (f) von Mises stress contours (MPa) in connection region for 1.00% drift of beam–column subassemblage studied (beam $W21\times142$ and column $W24\times160$). (g) Normal stress contours (MPa); (h) shear stress contours (MPa); and (i) von Mises stress contours (MPa) in connection region for 4.00% drift of beam–column subassemblage studied (beam $W21\times142$ and column $W24\times160$).

tabs welded to the column flange and bolt the beam web, to carry shear forces due to gravity loads in the extreme event of failure of the connection. The vertical rib plates located on the outer side of the cover plates, which are provided to transfer beam end shear to the column, also carry axial forces and thus have to be designed for the combined effect of flexure and shear. In actual construction, all the connection elements may be shop welded to the beam and the beam brought in position with the help the web tabs.

Proposed Design Procedure

Detailed finite element studies have shown that Euler–Bernoulli stress distribution is not applicable near the joint regions (Goel et al. 1996); near the joint, the beam shear is diverted towards the beam flanges resulting in stress concentration at the junction of the beam flanges and column face. Based on the results of that study, a connection configuration consisting of outer flange cover

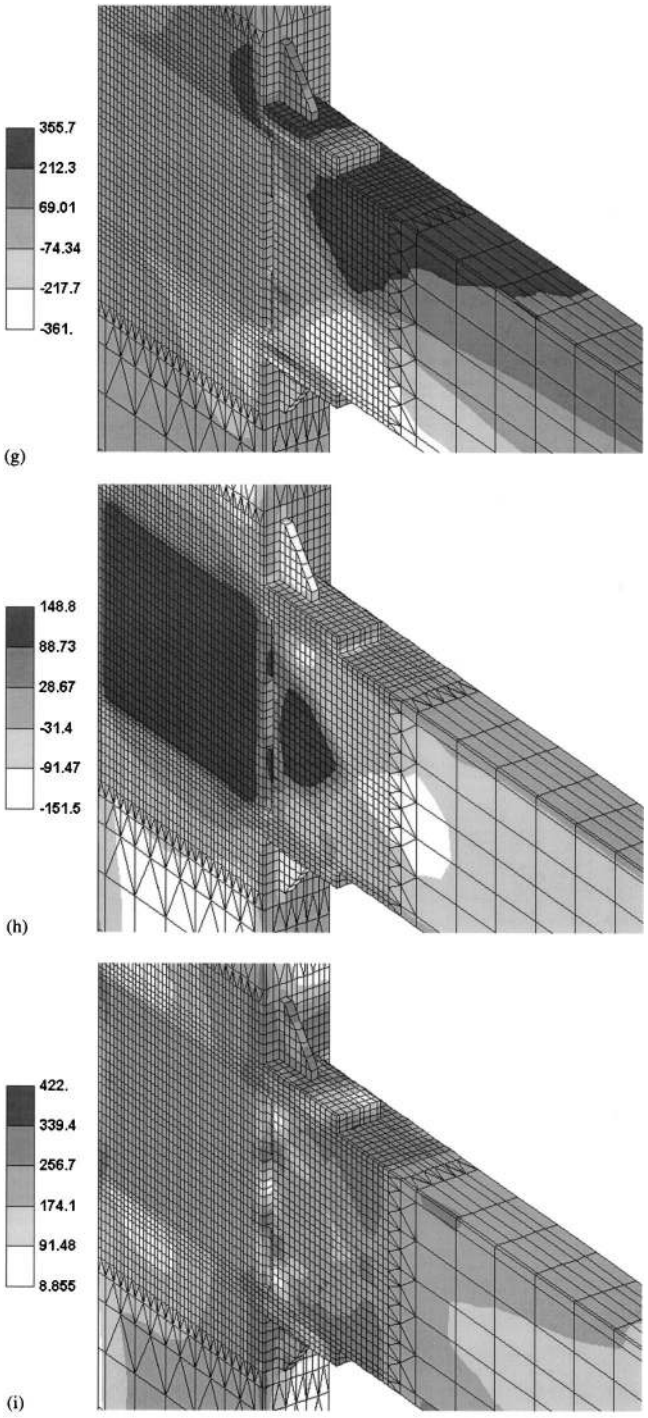

Fig. 6. (*Continued*)

plates and vertical rib plates (inner and outer) is used in this study (Fig. 3). The presence of the inner vertical rib plate also reduces the potential of crack initiation at the re-entrant cover plate to column flange junction, as observed in preliminary laboratory experiments (Moitra 2000). The step-wise procedure is presented hereunder for the design of connections elements. An example design calculation using this procedure for a beam of $W21\times142$ and a column of $W24\times160$ is presented in the Appendix.

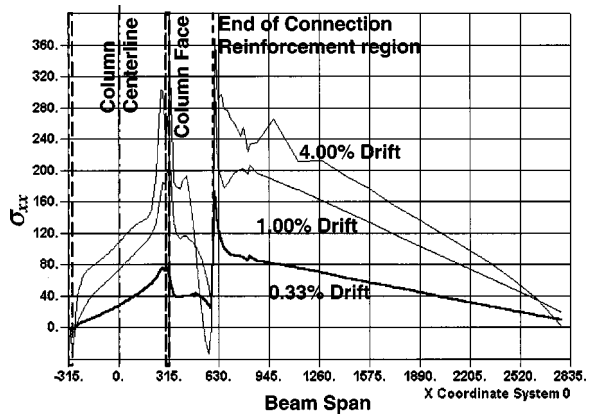

Fig. 7. Variation of normal stress (σ_{xx}) along beam top flange for one of beam–column subassemblages (beam $W21\times142$ and column $W24\times160$) analyzed

Part A: Moment Demand on Connections

1. Calculate the maximum probable moment M_{pr} to be transferred by the connection using

$$M_{\text{pr}}=C_{\text{pr}}R_yM_p \tag{4}$$

where C_{pr} and R_y=overstrength factors given in FEMA 350; and $M_p=F_yZ_b$.

2. Let the length l_c of the cover plate reinforcing the beam be one-half the depth of the beam ($d_b/2$). Assume the width, b_{cp}, of the cover plate such that the beam flange and the cover plate can be connected by a fillet weld

$$b_{\text{cp}}=b_{\text{bf}}-4t_{\text{bf}} \tag{5}$$

The fillet weld between beam flange and cover plate is a critical weld, and it is expected that its thickness will be larger than the beam flange thickness. Thus, the width of the cover plate is calculated such that a fillet weld of maximum size equal to twice the thickness of the beam flange can be deposited to connect the cover plate to the beam flange.

3. Calculate the length, L_0, of the shear link in the beam assuming that plastic hinges are located at either end of the beam at a distance of $0.5d_b$ from the end of the connection reinforcement region (Fig. 12) using

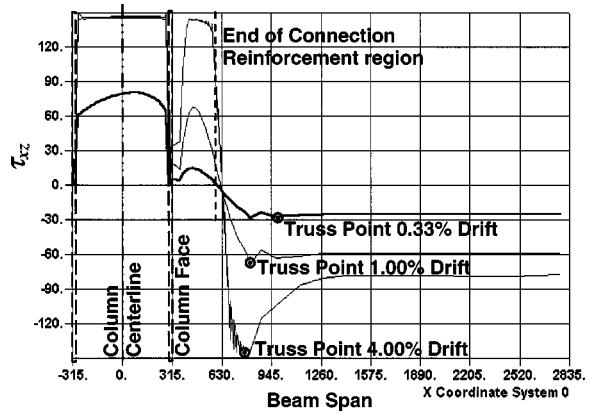

Fig. 8. Variation of shear stress (τ_{xz}) along beam centerline for one of beam–column subassemblages (beam $W21\times142$ and column $W24\times160$) analyzed

Table 2. Location of Truss Point, and Shear Stress in Beam and Column in Connection Region for 0.33% Drift

Sr. No.	Column	Beam	τ_{cpz}	τ_{bpz}	τ_b	τ_{cpz}/τ_b	τ_{bpz}/τ_b	τ_{tp}	l_t	l_t/d_b
1	W36×300	W33×240	113.6	25.4	78.1	1.455	0.325	81.2	395	0.464
2	d_c=932	W27×177	78.9	14.2	54.2	1.456	0.262	54.9	350	0.504
3		W21×142	47.23	12.2	28.7	1.646	0.425	29.1	338	0.620
4		W16×96	47.9	12.7	28.1	1.705	0.452	28.6	264	0.636
5		W12×58	31.1	20.5	18.3	1.699	1.120	18.8	177	0.571
6	W33×240	W27×144	100.5	14.0	57.9	1.736	0.242	67.0	371	0.535
7	d_c=851	W18×114	45.2	15.4	24.5	1.845	0.629	31.2	294	0.627
8		W12×58	34.5	22.7	20.9	1.651	1.086	20.8	207	0.668
9	W27×144	W24×160	69.7	7.1	26.3	2.650	0.270	26.6	393	0.566
10	d_c=694	W21×142	85.9	26.4	30.8	2.789	0.857	32.1	341	0.626
11		W16×96	61.6	16.5	23.4	2.632	0.705	24.4	293	0.706
12	W24×160	W21×142	80.4	14.8	25.4	3.165	0.583	28.3	406	0.745
13	d_c=628	W18×114	74.3	21.0	24.7	3.008	0.850	27.6	215	0.458
14		W12×58	40.4	18.1	17.0	2.376	1.065	19.0	231	0.745
15	W21×142	W21×142	91.8	19.0	25.2	3.643	0.754	26.1	325	0.596
16	d_c=545	W16×96	67.0	16.5	20.5	3.268	0.805	21.3	242	0.583
17	W18×114 d_c=469	W12×58	49.2	17.8	14.5	3.393	1.228	15.2	215	0.694
18	W16×96 d_c=415	W16×96	101.4	13.2	18.1	5.602	0.729	19.0	220	0.530

$$L_0 = L - \left(\frac{d_c}{2} + l_c + \frac{d_b}{2} + \frac{d_b}{2} + l_c + \frac{d_c}{2} \right) \tag{6}$$

where L=distance between the centerlines of the columns at the two ends of the beam and d_c=overall depth of the columns.

4. Calculate the probable maximum shear force, V_{pr}, on the connection, using

$$V_{pr} = \frac{2M_{pr}}{L_0} \tag{7}$$

5. Calculate the vertical shear force, V_d, and the horizontal pull

Table 3. Location of Truss Point, and Shear Stress in Beam and Column in Connection Region for 1% Drift

Sr. No.	Column	Beam	τ_{cpz}	τ_{bpz}	τ_b	τ_{cpz}/τ_b	τ_{bpz}/τ_b	τ_{tp}	l_t	l_t/d_b
1	W36×300	W33×240	144.6	96.5	108.7	1.330	0.888	145.3	217.0	0.255
2	d_c=932	W27×177	144.5	55.2	95.8	1.508	0.576	119.3	149.0	0.215
3		W21×142	143.1	84.8	79.3	1.805	1.069	144.1	130.0	0.239
4		W16×96	144.4	79.0	81.7	1.767	0.967	134.4	114.0	0.275
5		W12×58	91.7	95.5	52.9	1.733	1.805	78.7	85.0	0.274
6	W33×240	W27×144	144.7	81.7	93.6	1.546	0.873	145.0	144.0	0.207
7	d_c=851	W18×114	141.4	87.4	66.9	2.114	1.306	133.7	120.0	0.256
8		W12×58	91.3	92.8	51.7	1.766	1.795	76.1	119.0	0.384
9	W27×144	W24×160	145.3	58.8	76.6	1.897	0.768	77.36	395.0	0.569
10	d_c=694	W21×142	145.2	143.7	71.3	2.036	2.015	94.8	192.0	0.352
11		W16×96	144.6	69.7	60.0	2.410	1.162	85.4	143.0	0.345
12	W24×160	W21×142	145.0	67.8	59.1	2.453	1.147	67.6	282.0	0.517
13	d_c=628	W18×114	144.9	100.7	60.0	2.415	1.678	78.7	236.0	0.503
14		W12×58	116.6	63.3	48.3	2.414	1.311	57.14	154.0	0.497
15	W21×142	W21×142	145.1	91.3	54.1	2.682	1.688	56.1	320.0	0.587
16	d_c=545	W16×96	144.8	64.5	53.1	2.727	1.215	56.5	186.0	0.448
17	W18×114 d_c=469	W12×58	144.5	56.6	42.8	3.376	1.322	45.7	173.0	0.558
18	W16×96 d_c=415	W16×96	145.3	53.5	34.0	4.274	1.574	35.9	212.0	0.511

Table 4. Location of Truss Point, and Shear Stress in Beam and Column in Connection Region for 4% Drift

Sr. No.	Column	Beam	τ_{cpz}	τ_{bpz}	τ_b	τ_{cpz}/τ_b	τ_{bpz}/τ_b	τ_{tp}	l_t	l_t/d_b
1	$W36\times300$	$W33\times240$	144.9	138.9	120.7	1.20	1.15	154.9	209.0	0.246
2	$d_c=932$	$W27\times177$	144.7	103.6	110.9	1.30	0.93	152.8	161.8	0.233
3		$W21\times142$	144.5	91.6	86.8	1.66	1.06	145.9	185.0	0.339
4		$W16\times96$	144.5	97.5	88.5	1.63	1.10	144.9	184.0	0.443
5		$W12\times58$	101.9	143.6	58.3	1.75	2.46	110.3	144.0	0.465
6	$W33\times240$	$W27\times144$	145.1	123.8	107.0	1.36	1.16	152.4	199.0	0.287
7	$d_c=851$	$W18\times114$	144.6	102.9	74.9	1.93	1.37	143.8	200.0	0.426
8		$W12\times58$	101.8	143.5	56.8	1.79	2.53	110.5	168.0	0.542
9	$W27\times144$	$W24\times160$	153.7	144.5	95.2	1.61	1.52	146.1	196.0	0.282
10	$d_c=694$	$W21\times142$	146.3	144.8	81.0	1.81	1.79	143.2	255.0	0.468
11		$W16\times96$	144.8	120.2	67.6	2.14	1.78	130.8	189.0	0.455
12	$W24\times160$	$W21\times142$	149.9	144.6	78.6	1.91	1.84	145.3	209.0	0.383
13	$d_c=628$	$W18\times114$	145.8	144.6	69.7	2.09	2.07	141.8	165.0	0.352
14		$W12\times58$	134.0	127.1	54.9	2.44	2.32	107.4	195.0	0.629
15	$W21\times142$	$W21\times142$	156.4	145.0	74.1	2.11	1.96	144.6	114.0	0.209
16	$d_c=545$	$W16\times96$	146.0	144.5	63.6	2.30	2.27	134.4	186.0	0.448
17	$W18\times114$ $d_c=469$	$W12\times58$	144.9	144.2	51.8	2.80	2.78	108.9	183.0	0.590
18	$W16\times96$ $d_c=415$	$W16\times96$	162.3	84.3	52.1	3.12	1.62	54.9	269.0	0.648

force, T_d, for the top half of the connection using

$$V_d=\frac{V_{pr}}{2} \tag{8}$$

and

$$T_d=\frac{M_{pr}}{d_b}+\frac{V_{pr}}{2} \tag{9}$$

The second term in Eq. (9) is due to the moment amplification, which is the consequence of shifting the plastic hinge away from the column face and into the beam. These forces are calculated based on the truss model, which assumes that the beam shear is transferred to the column through the beam flanges and not through the beam web (Goel et al. 1996).

Part B: Design of Cover Plates

6. The weld between beam flange and cover plate is subjected to combined tension and shear (Fig. 3). Calculate the shear and tension for this weld, using

$$T_{wcp}=V_d \tag{10}$$

and

$$V_{wcp}=T_d-T_f \tag{11}$$

where $T_f=F_y b_{bf} t_{bf}$=capacity of beam flange using the minimum specified strength. It is expected that the yield strength of the steel is always higher than the minimum specified strength. Further, because the beam portion immediately after the connection reinforcement region is weaker than the reinforced region close to the column face, it is expected to yield first and prevent the inelasticity from entering the connection reinforcement region.

7. Since the length and width of cover plate are known, the length of weld between beam flange and cover plate is given by

$$l_{wcp}=2l_c+b_{cp} \tag{12}$$

8. Calculate the area of the fillet weld required to transfer the combined T_{wcp} and V_{wcp}, using

$$A_{wcp}=\sqrt{\frac{T_{wcp}^2+3V_{wcp}^2}{F_y^2}} \tag{13}$$

Calculate the thickness of this fillet weld, using

$$t_{wcp}=\frac{A_{wcp}}{l_{wcp}/\sqrt{2}} \tag{14}$$

The thickness of cover plate, t_{cp} is the same as the thickness of the fillet weld.

Part C: Design of Rib Plates

9. Assuming that the shear is transferred to the column by two outer rib plates, calculate the shear in each rib plate, using

$$V_{rp}=\frac{V_d}{2} \tag{15}$$

10. The fillet weld between the outer rib plates and cover plate is also under combined shear and tension. Calculate the magnitudes of these forces, using

$$T_{whrp}=V_{rp} \tag{16}$$

and

$$V_{whrp}=\frac{T_d-T_f-T_{cp}}{2} \tag{17}$$

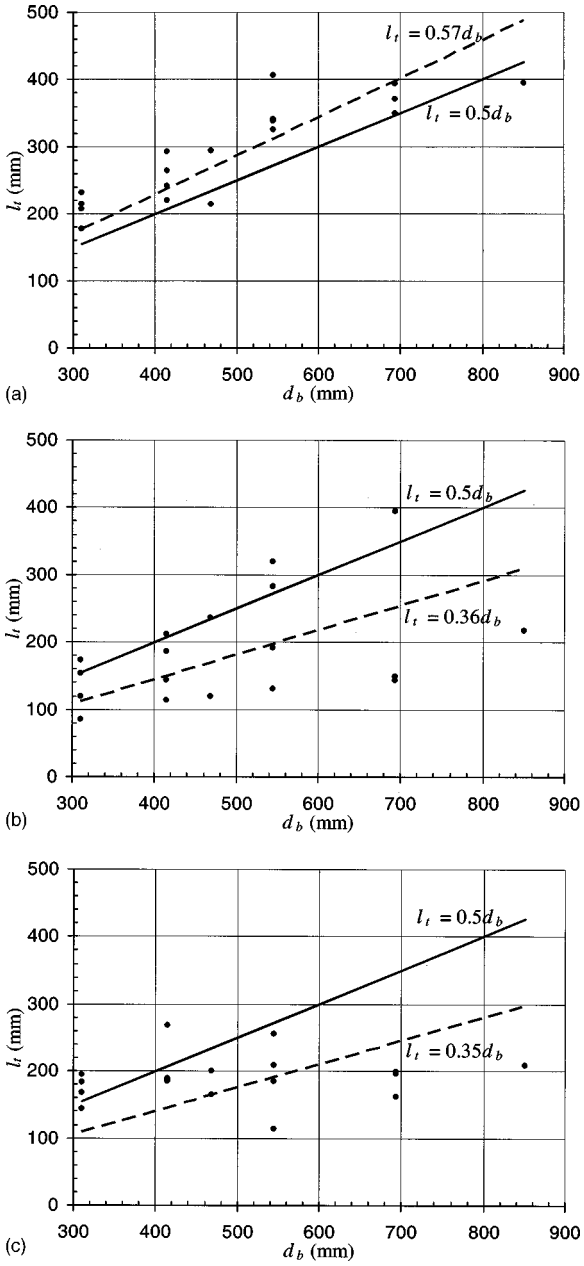

Fig. 9. Linear regression results for location of truss point at (a) 0.33% drift and $l_t=0.5d_b$; (b) 1.00% drift and $l_t=0.5d_b$; and (c) 4.00% drift and $l_t=0.5d_b$ proposed in this study to locate truss point to be used for calculation of connection design forces.

11. Calculate the area of fillet weld between cover plate and one rib plate, using

$$A_{\text{whrp}}=\sqrt{\frac{T_{\text{whrp}}^2+3V_{\text{whrp}}^2}{F_y^2}} \tag{18}$$

12. Assume the thickness of rib plate. The size, t_{whrp}, of fillet weld between the rib plate and the cover plate is equal to the thickness, t_{rp}, of the rib plate. Calculate the length of this fillet weld using

$$l_{\text{whrp}}=\frac{A_{\text{whrp}}}{t_{\text{whrp}}/\sqrt{2}} \tag{19}$$

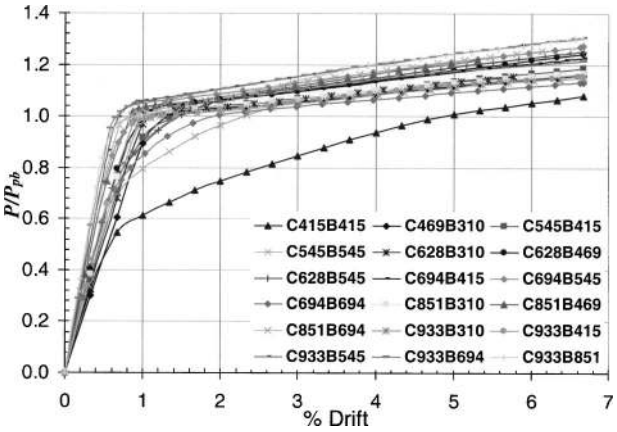

Fig. 10. Monotonic load versus drift curves for 18 subassemblages studied in this study (C933B545 in legend refers to column of depth 933 mm and beam of depth 545 mm)

Calculate the length of the rib plate using

$$l_{\text{rp}}=\frac{l_{\text{whrp}}}{2} \tag{20}$$

13. Calculate the horizontal tensile force for each rib plate using

$$T_{\text{rp}}=\frac{T_d-T_f-T_{\text{cp}}}{2} \tag{21}$$

where $T_{\text{cp}}=F_y b_{\text{cp}} t_{\text{cp}}$=capacity of cover plate using minimum specified strength.

14. Calculate the area of each rib plate to transfer combined shear and tension to the column using

$$A_{\text{rp}}=\sqrt{\frac{T_{\text{rp}}^2+3V_{\text{rp}}^2}{F_y^2}} \tag{22}$$

15. Assuming the thickness, t_{rp}, of the rib plate, calculate its height using

$$h_{\text{rp}}=\frac{A_{\text{rp}}}{t_{\text{rp}}} \tag{23}$$

Part E: Check for Moment Amplification

16. For the actual dimensions of the cover plate and vertical rib plates provided, calculate the capacities using

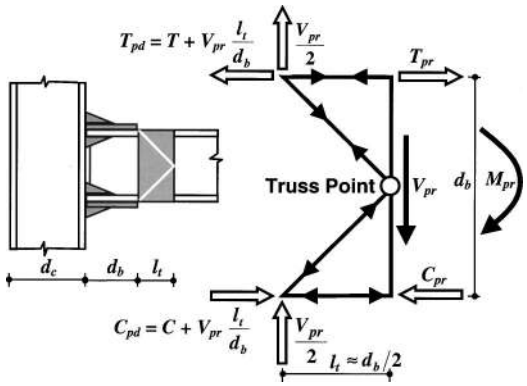

Fig. 11. Beam–column subassemblage showing location and configuration of improved truss model, and flow of forces for design of beam-to-column connection elements

$$T_{cp} = F_y b_{cp} t_{cp} \quad (24)$$

$$T_{rp} = F_y h_{rp} t_{rp} \quad (25)$$

and

$$V_{rp} = \frac{F_y}{\sqrt{3}} h_{rp} t_{rp} \quad (26)$$

17. Ensure that the connection capacity to resist the external moment is more than the moment demand on it including the effect of moment amplification using

$$(2T_{rp} + T_{cp} + T_f)(d_b + t_{cp}) \geq M_{pr} + V_{pr}(l_c + l_t) \quad (27)$$

Summary and Discussion

Detailed finite element models of 18 beam-to-column subassemblages are used to study the inelastic stress field in the connection region under large lateral deformations. An improved truss model is proposed to accurately represent the flow of forces near the connections of steel MRF beam-to-column joints. A noniterative procedure to rationally estimate the design forces on the different connection elements, namely cover plates and vertical rib plates, is proposed using the results of the nonlinear finite element analyses carried out in this study. The beam overstrength capacities are used to obtain the connection design forces. Cover plates are designed for pure axial forces, and the vertical rib plates are designed for combined axial and shear forces. The welds between the various connection components are designed for actual combined axial and shear stresses.

The improved truss model correctly locates the K-truss to start at the end of the connection reinforcement region. This is verified by nonlinear finite element analyses and is in contrast with the location of the truss assumed in the truss analogy model to start at the face of the column (within the connection reinforcement region) (Goel et al. 1997; Lee et al. 2000). The improved truss model also proposes the dimension of the K-truss as $d_b/2$, as against d_b assumed in the earlier truss analogy model.

The improved truss model presented in this paper gives realistic design forces for the connection elements. However, an experimental program to investigate the validity of the improved truss model is essential before it is formally accepted for the design of welded moment-shear connections in steel MRFs.

Acknowledgments

The finite element analysis of this study was carried out using the computer facilities at the Center for Excellence in Analysis and Design at the Indian Institute of Technology Madras, Madras. The writers thank the faculty of the Dept. of Civil Engineering at IIT Madras, in particular Professor A. Meher Prasad. The help provided by Mr. Vinu Unnithan and Mr. Ginu Unnithan, graduate students at the Dept. of Civil Engineering, IIT Madras, is gratefully acknowledged.

Appendix. Design Example Using Proposed Procedure

An example design calculation using the procedure described in this paper for beam of $W21\times142$ and column of $W24\times160$ is listed below

$$d_b = 545 \text{ mm}; \quad b_{bf} = 334 \text{ mm}$$

$$t_{bf} = 28 \text{ mm}; \quad d_c = 628 \text{ mm}$$

$$Z_b = 357 \text{ in.}^4 = 5.85\times10^6 \text{ mm}^4$$

$$M_{pb} = 1{,}463 \text{ kN m}$$

Part A: Moment Demand on Connections

1. $$M_{pr} = C_{pr} R_y M_p = 2{,}765 \text{ kN m}$$

$$C_{pr} = \frac{F_u + F_y}{2F_y} = 1.26 \quad \text{for } F_u = 380 \text{ MPa}$$

and

$$F_y = 250 \text{ MPa}$$

2. $l_c = \mathbf{270\ mm}$; $b_{cp} = b_{bf} - 4t_{bf} = 222$, say $\mathbf{220\ mm}$

3. $$L_0 = L - \left(\frac{d_c}{2} + l_c + \frac{d_b}{2} + \frac{d_b}{2} + l_c + \frac{d_c}{2}\right) = 4{,}287 \text{ mm}$$

4. $$V_{pr} = \frac{2M_{pr}}{L_0} = 1{,}290 \text{ kN}$$

5. $$V_d = \frac{V_{pr}}{2} = 645 \text{ kN}; \quad T_d = \frac{M_{pr}}{d_b} + \frac{V_{pr}}{2} = 5{,}717 \text{ kN m}$$

Part B: Design of Cover Plates

6. $$T_{wcp} = V_d = 645 \text{ mm}; \quad T_f = F_y b_{bf} t_{bf} = 2{,}338 \text{ kN}$$

$$V_{wcp} = T_d - T_f = 3{,}379 \text{ kN}$$

7. $$l_{wcp} = 2l_c + b_{cp} = 760 \text{ mm}$$

8. $$A_{wcp} = \sqrt{\frac{T_{wcp}^2 + 3V_{wcp}^2}{F_y^2}} = 23{,}550 \text{ mm}^2$$

$$t_{cp} = t_{wcp} = \frac{A_{wcp}}{l_{wcp}/\sqrt{2}} = 43.82, \text{ say } \mathbf{45\ mm}$$

Part C: Design of Rib Plates

9. $$V_{rp} = \frac{V_d}{2} = 322 \text{ kN}$$

10. $$T_{whrp} = V_{rp} = 322 \text{ kN}$$

$$V_{whrp} = \frac{T_d - T_f - T_{cp}}{2} = 452 \text{ kN}$$

11. $$A_{whrp} = \sqrt{\frac{T_{whrp}^2 + 3V_{whrp}^2}{F_y^2}} = 3{,}386 \text{ mm}^2$$

12. $$l_{whrp} = \frac{A_{whrp}}{t_{whrp}/\sqrt{2}} = 239 \text{ mm}$$

$$l_{rp} = \frac{l_{whrp}}{2} = 119.7, \text{ say } \mathbf{120\ mm}$$

13. $$T_{cp} = F_y b_{cp} t_{cp} = 2{,}475 \text{ kN}$$

$$T_{rp} = \frac{T_d - T_f - T_{cp}}{2} = 452 \text{ kN}$$

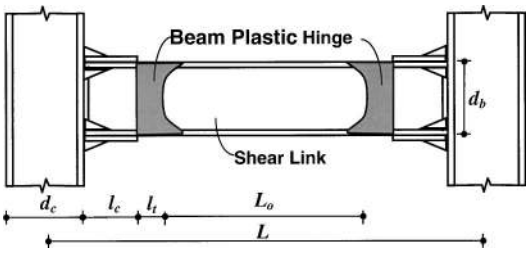

Fig. 12. Location of beam plastic hinges at end of connection reinforcement region in typical steel beam–column frame

14. $$A_{rp}=\sqrt{\frac{T_{rp}^2+3V_{rp}^2}{F_y^2}}=2{,}873\ \text{mm}^2$$

15. $t_{rp}=$ **20 mm**; $h_{rp}=\frac{A_{rp}}{t_{rp}}=143.7$, say **150 mm**

16. $$T_{cp}=F_y b_{cp} t_{cp}=2{,}475\ \text{kN}$$
$$T_{rp}=F_y h_{rp} t_{rp}=750\ \text{kN}$$
$$V_{rp}=\frac{F_y}{\sqrt{3}} h_{rp} t_{rp} 433\ \text{kN}$$

17. $$(2T_{rp}+T_{cp}+T_f)(d_b+t_{cp})\geq M_{pr}+V_{pr}(l_c+l_t)$$
$$3{,}724\ \text{kN m}\geq 703\ \text{kN m}\quad \therefore\text{OK.}$$

Adopt: **Cover Plate**:**270 mm×220 mm×45 mm**
Rib Plate: **120 mm×145 mm×20 mm**

Notation

The following symbols are used in this paper:

A_{rp} = area of rib plate;
A_{wcp} = area of fillet weld between beam flange and cover plate;
A_{whrp} = area of fillet weld between cover plate and rib plate;
B = breadth;
b_{bf} = width of beam flange;
b_{cf} = width of column flange;
b_{cp} = width of cover plate;
C = compressive force in beam bottom flange;
C_{pd} = connection design horizontal compressive force in bottom connection element;
C_{pr} = peak connection strength factor (FEMA 2000); probable maximum compressive force capacity of beam;
d_b = depth of beam;
d_c = depth of column;
F_u = ultimate strength of beam material;
F_y = yield strength of beam material;
h_{rp} = height of rib plate;
L = center to center distance between columns at end of beam; length;
L_0 = length of shear link, length of beam between plastic hinges;
l_c = length of reinforced region of beam, length of cover plate;
l_{rp} = length of rib plate;
l_t = distance of truss point from end of connection reinforcement region;
l_{wcp} = length of fillet weld between beam flange and cover plate;
l_{whrp} = length of fillet weld between cover plate and rib plate;
M = beam moment;
M_p = plastic moment;
M_{pb} = beam plastic moment;
M_{pc} = column plastic moment;
M_{pr} = moment from beam capacity;
P = beam transverse load;
P_{pb} = beam transverse load corresponding to M_{pb};
R_y = material overstrength factor;
T = tensile force in beam top flange; thickness;
T_{cp} = tensile capacity of cover plate;
T_d = design axial force for top or bottom half of connection;
T_f = elastic axial capacity of beam flange;
T_{pr} = total horizontal connection design force;
T_{rp} = design axial force for rib plate;
T_{wcp} = tensile force in fillet weld between beam flange and cover plate;
T_{whrp} = design axial force for fillet weld between cover plate and rib plate;
t_{bf} = thickness of beam flange;
t_{bw} = thickness of beam web;
t_{cp} = thickness of cover plate;
t_{rp} = thickness of rib plate;
t_{wcp} = thickness of fillet weld between beam flange and cover plate;
t_{whrp} = thickness of fillet weld between cover plate and rib plate;
V = shear force;
V_d = design shear force for top or bottom half of connection;
V_{pd} = connection design shear force;
V_{pr} = maximum shear force on connection;
V_{rp} = design shear force for rib plate;
V_{wcp} = shear force in fillet weld between beam flange and cover plate;
V_{whrp} = design shear force for fillet weld between cover plate and rib plate;
Z_b = plastic section modulus of beam;
Δ = beam tip displacement;
σ_{xx} = normal stress;
σ_y = yield stress of steel;
τ_b = maximum shear stress in unreinforced portion of beam;
τ_{bpz} = maximum shear stress in reinforced section of beam;
τ_{cpz} = shear stress in column panel zone;
τ_{tp} = shear stress in beam web at truss point; and
τ_{xz} = shear stress.

References

Englehardt, M. D., and Sabol, T. A. (1998). "Reinforcing of steel moment connections with cover plates: benefits and limitations." *Engineering structures*, Vol. 20, Elsevier Science, New York, 249–260.

EQE. (1994). "The January 17, 1994 Northridge, California Earthquake." *An EQE Summary Report March*, EQE International, San Francisco.

Federal Emergency Management Agency (FEMA). (1995). "Interim guidelines: Evaluation, repair, modification and design of welded steel

moment frame structures.'' *Rep. No. SAC-95-02*, Washington, D.C.
Federal Emergency Management Agency (FEMA). (2000). ''Recommended seismic design criteria for new steel moment-frame buildings.'' *FEMA 350*, SAC Joint Venture, Calif.
Goel, S. C., Stojadinovic, B., and Lee, H. K. (1996). ''A new look at steel moment connections.'' *Rep. No. UMCEE 96-19*, The Univ. of Michigan College of Engineering.
Goel, S. C., Stojadinovic, B., and Lee, H. K. (1997). ''Truss analogy for steel moment connections.'' *Eng. J.,* Second Quarter, 43–53.
Hibbitt, Karlsson & Sorensen, Inc. (HKS). (1996). *ABAQUS: User information manual; revision 5.5*, HKS, Calif.
Krawinkler, H., and Popov, E. P. (1982). ''Seismic behavior of moment connections and joints.'' *ASCE J. Struct. Div.,* 108(2), 373–391.
Lee, K. H., Goel, S. C., and Stojadiovic, B. (1998). ''Boundary effects in welded steel moment connections.'' *Proc., 6th U.S. National Conf. on Earthquake Engineering*.
Lee, K. H., Goel, S. C., and Stojadiovic, B. (2000). ''Boundary effects in steel moment connections.'' Paper No. 1098, *Proc., 12th World Conf. on Earthquake Engineering*, Auckland, New Zealand.
Malley, J. O. (1998). ''SAC project: summary of phase 1 testing investigation results.'' *Eng. Struct.,* 20(4–6), 300–309.
Miller, D. K. (1998). ''Lessons learned from the Northridge Earthquake.'' *Eng. Struct.,* 20(4–6), 249–260.
Moitra, A. (2000). ''Experimental investigation of cyclic response of reinforced connections for earthquake resistant steel MRFs.'' Master of Technology thesis, Indian Institute of Technology Kanpur, India.
National Institute of Standards and Technology (NIST). (1994). ''1994 Northridge earthquake: performance of structures, lifelines, and fire protection systems.'' *NIST Special Publication 862 (ICSSC TR14)*, United States Dept. of Commerce and Technology Administration, Gaithersburg, Md.
Roeder, C. W. (1998). ''Design models for moment resisting steel construction.'' *Structural engineering worldwide*, Elsevier, New York.
Sabol, T. A., Englehardt, M. D., Aha, A., and Frank, K. H. (1996). ''Overview of the Northridge moment connection test program.'' *Proc., 11th World Conf. on Earthquake Engineering*, Elsevier Science, New York.
Saunders, C. M. (1998). ''Design criteria for steel moment resisting frame buildings.'' *Structural engineering worldwide*, Elsevier, New York.
Schneider, S. P., and Amidi, A. (1998). ''Seismic behavior of steel frames with deformable panel zones.'' *J. Struct. Eng.,* 124(1), 35–42.